Contribution of neuroblastoma-derived exosomes to the production of pro-tumorigenic signals by bone marrow mesenchymal stromal cells

Rie Nakata, Hiroyuki Shimada, G. Esteban Esteban Fernandez, Rob Fanter, Muller Fabbri, Jemily Malvar, Pascale Zimmermann, Yves A Declerck

HAL Id: hal-01784516
https://amu.hal.science/hal-01784516

Submitted on 3 May 2018

Taylor & Francis
Taylor & Francis Group

RESEARCH ARTICLE

Contribution of neuroblastoma-derived exosomes to the production of pro-tumorigenic signals by bone marrow mesenchymal stromal cells

Rie Nakata[a,b,c], Hiroyuki Shimada[a,d], G. Esteban Fernandez[a], Rob Fanter [a], Muller Fabbri[a,b,c,e], Jemily Malvar [a,b], Pascale Zimmermann [g] and Yves A. DeClerck [a,b,c,f]

[a]The Saban Research Institute of Children's Hospital Los Angeles, University of Southern California, Los Angeles, CA, USA; [b]Division of Hematology, Oncology, and Blood & Marrow Transplantation, University of Southern California, Los Angeles, CA, USA; [c]Department of Pediatrics, University of Southern California, Los Angeles, CA, USA; [d]Department of Pathology and Laboratory Medicine, University of Southern California, Los Angeles, CA, USA; [e]Department of Molecular Microbiology and Immunology, University of Southern California, Los Angeles, CA, USA; [f]Department of Biochemistry and Molecular Biology, Keck School of Medicine, University of Southern California, Los Angeles, CA, USA; [g]Centre de Recherche en Cancérologie de Marseille (CRCM), Inserm, U1068-CNRS UMR7258, Aix-Marseille Université, Institut Paoli-Calmettes, Marseille, France

ABSTRACT

The bone marrow (BM) niche is a microenvironment promoting survival, dormancy and therapeutic resistance in tumor cells. Central to this function are mesenchymal stromal cells (MSCs). Here, using neuroblastoma (NB) as a model, we demonstrate that NB cells release an extracellular vesicle (EVs) whose protein cargo is enriched in exosomal proteins but lacks cytokines and chemokines. Using three different purification methods, we then demonstrate that NB-derived exosomes were captured by MSCs and induced the production of pro-tumorigenic cytokines and chemokines, including interleukin-6 (IL-6), IL-8/CXCL8, vascular endothelial cell growth factor and monocyte-chemotactic protein-1, with exosomes prepared by size exclusion chromatography having the highest activity. We found no correlation between the IL-6 and IL-8/CXCL8 stimulatory activity of exosomes from eight NB cell lines and their origin, degree of MYCN amplification, drug resistance and disease status. We then demonstrate that the uptake of NB exosomes by MSCs was associated with a rapid increase in ERK1/2 and AKT activation, and that blocking ERK1/2 but not AKT activation inhibited the IL-6 and IL-8/CXCL8 production by MSCs without affecting exosome uptake. Thus, we describe a new mechanism by which NB cells induce in MSCs an inflammatory reaction that contributes to a favorable microenvironment in the BM.

Introduction

Because of its rich composition in pluripotent and migratory cells [1] the bone marrow (BM) actively contributes to the tumour microenvironment (TME) [2]. Locally, the BM attracts circulating tumour cells and provides them with a sanctuary against the injury of therapies promoting dormancy and the establishment of minimal residual disease (MRD) [3–5]. Central to this function are mesenchymal stromal cells (MSCs), progenitors of osteoblasts, adipocytes and chondroblasts that contribute to the BM niche [6,7]. MSCs and derived cells can be polarised towards a tumour-suppressive or tumour-promoting activity [8]. This latter function includes a suppressive activity on the immune system as well as the ability to promote tumour cell growth, migration and metastasis [9], and drug resistance [10] through the production of soluble cytokines and chemokines. The mechanisms involved in the activation and polarisation of MSCs are not well understood but they include the production by tumour cells of soluble factors like interferon γ, tumour necrosis factor α and IL-1β [8,11,12].

Among soluble products released by tumour cells are extracellular vesicles (EVs), that due to their ability to exchange lipids, proteins and nucleic acids between cells, have been recognised as playing a central role in cell–cell communication [13–15]. EVs are a heterogeneous group of vesicular structures with diameters ranging from 20 to 5000 nm, classified in three groups [13]: exosomes originating from endosomes, microvesicles (MVs) generated by the budding of the plasma membrane and apoptotic bodies released by dying cells. Exosomes are generated by intraluminal budding of endosomal membranes into multivesicular bodies (MVBs, aka late endosomes) and are released in the extracellular space when MVBs fuse with the plasma

membrane instead of trafficking towards lysosomes for degradation [16].

The role of exosomes in the communication between cancer cells and stromal cells in the TME has been the subject of increased interest over the past decade but much remains to be learned about their exact function [17,18]. Evidence, however, points to a role in inducing a microenvironment that is favourable to cancer progression and in promoting immune escape [19,20]. Tumour-derived exosomes also stimulate angiogenesis and metastasis [21,22], and contribute to the pre-metastatic niche by educating BM-derived progenitor cells [23].

For our studies we selected neuroblastoma (NB), the second most common solid tumour in children, because of its high incidence of BM and bone metastasis [24,25], the availability of established cell lines derived from the BM of patients with metastatic disease and previous evidence from our laboratory that NB cells activate MSCs [26]. Here we demonstrate that exosomes released by NB cells contribute with other soluble factors to the polarisation of MSCs towards a pro-tumorigenic phenotype by stimulating in an ERK1/2-dependent manner the release of cytokines and chemokines favourable to tumour cells.

Methods

Cells

Human NB cell lines CHLA-255, CHLA-90, SK-N-BE (2), and LAN-6 were kindly provided by Dr C.P. Reynolds (Texas Tech University, Lubbock, TX) and Dr R. Seeger (Children's Hospital Los Angeles, Los Angeles, CA), and the NB-19 cell line was purchased from RIKEN (Ibaraki, Japan). SK-N-SH, SK-N-RA, SK-SY-5Y and IMR32 cells were obtained from the American Type Culture Collection. Cell line authentication was done by genotype analysis using AmpFISTR® Identifiler® PCR Amplification Kit and Gene Mapper ID v3.2 (Applied Biosystems). Human NB cells were cultured in Iscove's Modified Dulbecco's Medium (IMDM) (Cell Culture Core, USC Norris Comprehensive Cancer Center, Los Angeles, CA) supplemented with 10% (v/v) foetal bovine serum (FBS, Omega Scientific), penicillin (100 units/ml) and streptomycin (0.1 mg/ml) (Gibco), and 0.1% (v/v) insulin, transferrin, selenium (ITS) Universal Culture Supplements (BD Biosciences). Human BM-derived MSCs were purchased from AllCells or isolated in our laboratory from the BM of patients with NB using a previously published protocol [10]. Cells were maintained in Dulbecco's Modified Eagle Medium (DMEM)

(Corning) supplemented with 15% (v/v) FBS, and L-glutamine (4 mM) (Gibco) for a maximum of eight passages. These cells were characterised according to the criteria established by the International Society for Cellular Therapy [27], and tested positive by flow cytometry for the presence of CD105, CD90 and CD73 and negative for hematopoietic (CD34), myeloid (CD45, CD13), endothelial (CD31, VEGFR2) and lymphoid (CD4, CD8) markers. These cells maintained the ability to differentiate into adipocytes, osteoblasts and chondrocytes when cultured in the appropriate media [28]. Because of their typical fibroblast-like morphology and in the absence of evidence that they are true stem cells, we designated these cells MSCs rather than mesenchymal stem cells, as recommended [27]. Human foreskin fibroblast cells were provided by Dr T.L. Tuan (CHLA) and cultured in DMEM supplemented with 10% (v/v) FBS, and L-glutamine (4 mM). The absence of contamination of the cultures with *Mycoplasma* was verified using MycoAlert™ PLUS Mycoplasma Detection Kit (Lonza).

Reagents

PKH67 green fluorescent cell linker kit was obtained from Sigma, trametinib from LC Laboratories and MK-2206 from Selleck Chemicals. Liposomes were obtained from Encapsula NanoSciences. The following primary antibodies were used for western blot analysis: anti-CD63 (EXOAB-CD63A-1) antibody was purchased from System Biosciences, anti-ALIX (ab117600), anti-CD81 (ab109201), anti-GM130 (ab5249), anti-chromogranin-A (ab68271) and anti-calnexin (ab22595) antibodies were obtained from Abcam, and anti-actin (A2228) antibody from Sigma-Aldrich). Anti-Gal-3BP (AF2226) and anti-VEGF (AF293) antibodies were obtained from R&D. Anti-STAT3 (4904), anti-phosphoSTAT3 (9131), anti-ERK (9102), anti-phosphoERK (7101), anti-Akt (9272), anti-phosphoAkt (4060), anti-NFκB/p65 (4764), anti-phosphoNFκB (3033) and anti-HMGB1 (6893) antibodies were purchased from Cell Signaling. Unless specified, these primary antibodies were used at a 1:1000 dilution. The rabbit polyclonal antibody against syndecan binding protein (SDBP)/syntenin-1 (dilution 1:3000) was described earlier [29] and mouse hybridoma antibodies against human CD63 and CD81 (dilution 1:2,000) were provided by Dr E. Rubinstein (Villejuif, Paris University, France). The following secondary antibodies were purchased from LI-COR Biosciences and used at a 1:10,000 dilution: IRDye® 800CW goat anti-Rabbit IgG, IRDye® 680RD goat anti-Mouse IgG and IRDye® 680RD donkey anti-Goat IgG.

Conditioned media (CM)

Cells were washed with PBS twice and the medium changed to serum-free IMDM supplemented with 0.01% (v/v) ITS. The absence of FBS allowed us to avoid potential contamination with bovine proteins, bovine exosomes and bovine lipoproteins. We found that the absence of FBS did not affect cell viability and apoptosis over 48 and 72 h. It had no effect on the number of EVs released by CHLA-255 cells and it increased EV production in SK-N-BE(2) cells as reported by others [30] (Supplemental Figure 1). CM was collected after 48–72 h and centrifuged at 2000*g* for 4 min to remove cells, cell debris and apoptotic bodies before being further processed.

Preparations of EVs and exosomes

Initial preparations of EVs were obtained from CM filtrated through a 0.2 μm cellulose acetate membrane (VWR) and concentrated 10–50 fold on a 100K MWCO concentrator (Thermo Scientific Pierce) before being

pelleted by ExoQuick-TC (System Biosciences) and resuspended in PBS. These preparations were designated eqEV. Preparations of EVs with characteristics of exosomes were obtained by differential ultracentrifugation (DUC), OptiPrep (Sigma-Aldrich) density gradient centrifugation (ODGC) or size exclusion chromatography (SEC) [31]. The presence of exosomes in all preparations was defined by the detection by western blot analysis of the tetraspanins CD63, CD9 and CD81 (not exclusively present in exosomes) and syntenin-1 and ALIX being bona-fide markers of exosomes because of their involvement in exosome biogenesis [32,33], in the absence of calnexin and GM-130 (endoplasmic reticulum and mitochondrial markers respectively) [34]. EVs in these preparations were also examined for size by nanoparticle tracking analysis (NTA) and electron microscopy (EM). For DUC, CM was centrifuged at 2000*g* for 5 min to remove floating cells and apoptotic bodies. The supernatant was then collected and ultracentrifuged at 10,000*g* (Eppendorf 5810 R centrifuge with F-34–6-38 rotor) at 4°C for 30 min to eliminate MVs (designated duc10kEVs). The supernatant
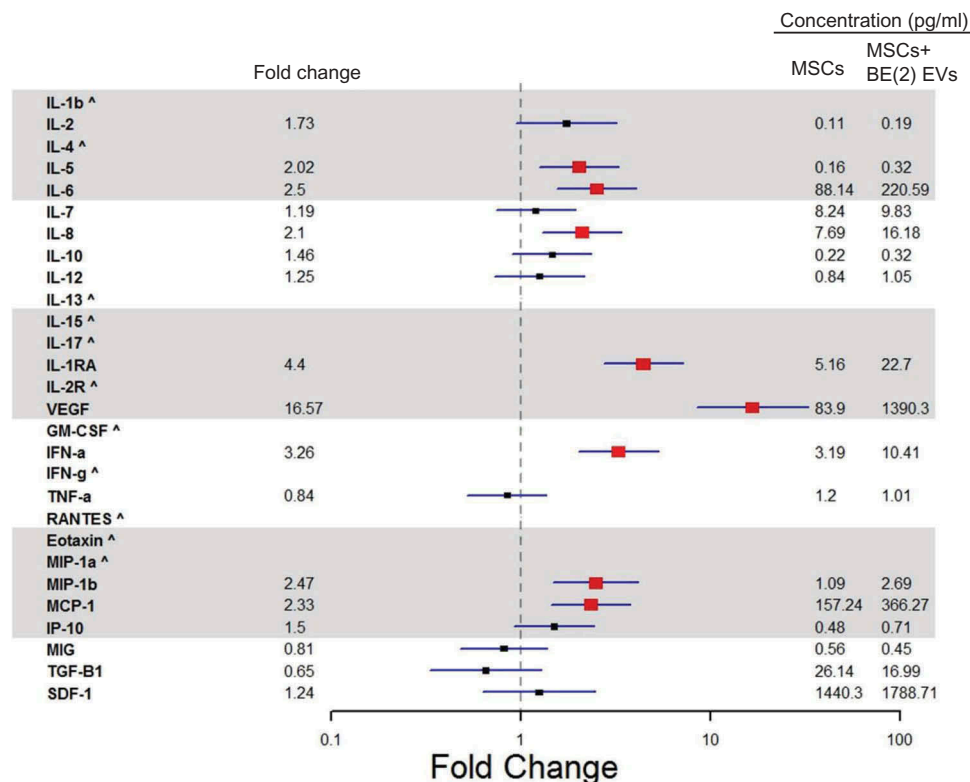
Figure 1. NB-derived eqEVs stimulate the expression of pro-tumorigenic cytokines and chemokines in MSCs. MSCs (3 × 10⁴ cells/well) were exposed for 24 h to eqEVs (2.5 μg/well) obtained from SK-N-BE[2] cells. The medium was tested for the presence of 28 cytokines and chemokines using a Luminex bead panel and ELISA (VEGF-A, SDF-1 and TGFβ). The data were generated from triplicate samples in a single experiment. Means and 95% confidence interval of fold changes are shown in box and lines, respectively; red box indicates significant (*p* < 0.05) fold changes for each comparison versus MSCs. Fold changes are displayed on the left, while the concentrations of cytokines and chemokines in pg/ml are shown on the right-hand side of the figure. The ^ indicates cases in which all observations under one condition group are censored. Similar data were obtained with CHLA-255 and NB-19 cells (Supplemental Figures 2 and 3).

was then collected and recentrifuged at 100,000*g* for 3 h at 4°C (SW32Ti rotor, Optima XE-90 ultracentrifuge, Beckman). The pellet (designated duc100kEVs) was resuspended in 10.5 ml of PBS, centrifuged at 100,000*g* for 1 h, resuspended in 25–50 µl in PBS and stored at −20°C prior to testing. For ODGC, after centrifugation at 10,000*g*, the CM was concentrated on a 100K MWCO concentrator, loaded on the top of an iodixanol (OptiPrep™) gradient (2.5 ml of 5% (w/v), 3.0 ml of 20% and 4.8 ml of 30% in PBS), and separated on the basis of buoyancy by ultracentrifugation at 100,000*g* at 4°C for 16 h in a SW40Ti rotor. Individual fractions of 1 ml were collected from the top, diluted in 10 ml of PBS and recentrifuged at 100,000*g* for 2 h at 4°C. The pellets were resuspended in 25–50 µl of PBS and stored at −20°C before being analysed. EVs (designated odgcEVs) with characteristics of exosomes were present in fractions 4–6 (peak 2; density of 1.02–1.1 g/ml). For SEC the concentrated CM was loaded on a Sepharose CL-2B column (0.8 cm² cross diameter x 17 cm length) and eluted in PBS at a rate of 0.5 ml/min. Individual fractions of 2 ml were collected. EVs with characteristics of exosomes were present in fractions 3 to 5 (designated secEVs in peak 1) and were concentrated on a 100K MWCO concentrator. The absence of endotoxin in the CM and in exosome preparations was verified by EndoLISA® endotoxin detection assay (Hyglos GmbH). In all samples, endotoxin levels were <0.02 ng/ml.

Transmission electron microscopy (TEM)

The pellets containing exosomes were fixed with 2% (w/v) glutaraldehyde (Ted Pella Inc.) and post-fixed with 1% (w/v) osmium tetroxide (Ted Pella Inc.). After being dehydrated and embedded in Eponate 12 Resin (Ted Pella Inc.), ultra-thin sections of the samples were cut, placed on carbon coated grids and stained in 5% (w/v) uranyl acetate solution and 3% (w/v) lead solution (Ted Pella Inc.). Digital images of the samples were examined and recorded using a Morgagni 268 transmission electron microscope (Field Emission Inc.).

Nanoparticle tracking analysis (NTA)

NTA of EVs was done using a NanoSight NS300 instrument (Malvern Instruments). For data acquisition, samples were diluted in PBS to a particle concentration between 2×10^8 and 1×10^9 particles/ml and examined at a temperature of 20–25°C with a camera level of 13 and a gain of 250–300 over 30 or 60 s in triplicate. For data analysis, a detection threshold of 3 was used and Blur/track length/expected size were on AUTO. Data were analysed with the NTA version 2.3.

Western blot

Sodium dodecyl sulfate (SDS) polyacrylamide gel electrophoresis (PAGE) was performed on 4–15% (w/v) gradient acrylamide gels (TCX™, BioRad). Proteins were detected with a near-infrared fluorescence imaging system (Odyssey Imager LI-COR Biosciences). Levels of phospho-proteins, normalised to total protein levels, were determined by analysis of fluorescence intensity using Image Studio V3.1 software.

Proteomics analysis

For each analysis, 10 µg of proteins from eqEV preparations were separated by SDS-PAGE and digested in the gels overnight with trypsin at 37°C (Promega, #V5111). The generated peptides were purified via Varian C18 OMIX tips (Agilent Technologies, Santa Clara, CA) and analysed using an Eksigent nano LC-2D (SCIEX) coupled to a Thermo Orbitrap XL tandem mass spectrometer. Proteins were identified from raw MS data using Proteome Discoverer™ (Thermo) software packages in conjunction with the UniProt human proteome. Relative protein quantitation was performed in Scaffold (Proteome Software) according to number of assigned spectra, using 95% minimum protein and peptide identification probabilities and a minimum peptide count of two. The data were deposited in the Vesiclepedia/ExoCarta [35] and the EVpedia [36] data bases. Enrichment analysis was performed using the FunRich open access network analysis tool [37].

Chemokines and cytokines analysis

MSCs were plated at 3×10^4 cells per well in 96-well tissue culture plates in 100 µl of FBS-free medium containing NB-derived EVs or exosomes (2.5–10 µg/well) for 24 h. The presence of human cytokines and chemokines in the media was determined using a human Cytokine Magnetic 25-Plex Panel (Invitrogen) according to the manufacturer's protocol. The data were acquired with a Luminex®-200 instrument (Luminex® Corporation). Cytokine concentrations were determined by referring to a standard curve and expressed in pg/ml using XPONENT software (Luminex® Corporation). The presence of some cytokines (IL-6, IL-8/CXCL-8, VEGF, MCP-1/CCL2, SDF1, TGF-β) was also quantified by ELISA using a DuoSet ELISA Kit (R&D Systems).

Exosome membrane labelling and cell microscopy

EV membrane labelling was done using the PKH67 green fluorescent cell linker kit (Sigma-Aldrich). In

brief, duc100kEVs or liposomes (Encapsome, Encapsula NanoSciences LLC) were mixed in 200 µl of PBS with an equal volume of diluent C and PKH67 mix (1 µl) and incubated for 4 min at room temperature. The reaction was stopped by the addition of bovine serum albumin (BSA) at a final concentration of 0.5% (w/v) for 1 min. The PKH67 stained EVs were then purified by ODGC as described above, collected, diluted in PBS, centrifuged at 100,000g for 2 h and resuspended in PBS. Human MSCs (3×10^4 cells/well) were seeded in 8-well chambers overnight and incubated with PKH67-labelled exosomes (0.5-5×10^9 particles/ml, 0.3 ml/well) for 24 h. The cells were washed twice in PBS, fixed in 4% (w/v) formaldehyde for 15 min, rinsed with PBS twice and mounted with VECTASHIELD® mounting medium containing 4,6-diamino-2-phenylindole (DAPI); Vector Laboratories) before being examined under fluorescence microscopy (Leica DM RXA Upright Fluorescence Microscope). For confocal microscopy, the cells incubated with PKH67-labelled exosomes were washed twice in PBS, stained with FM4-64FX (100 µg/ml, Thermo Fisher Scientific) for 1 min on ice and washed twice in PBS before being examined. Confocal z-stacks were acquired with an LSM 710 system mounted on an Axio Observer.Z1 microscope equipped with a C-APOCHROMAT 40x/1.2 water-immersion lens (Carl Zeiss Microscopy). Fluorescence excitation was achieved with a laser wavelength of 488 nm. Fluorescence emission was detected using wavelengths of 490–580 nm and 650–758 nm for PKH67 and FM4-64FX, respectively. Raw z-stacks were deconvoluted with AutoQuant AutoDeblur ver. X1.4.1 software by applying the Adaptive PSF (blind) algorithm with default parameters (Media Cybernetics). Final images were generated by manually adjusting brightness/contrast, cropping and creating orthogonal projections with ZEN LE software (Carl Zeiss Microscopy).

Statistics

Two-sample t-tests were utilised to evaluate pairwise comparisons of the different experimental conditions. Unless otherwise stated, p-values refer to two-sided tests. Statistical analyses were completed using the statistical software R, Stata and GraphPad Prism 6. Results from the Luminex assays were log transformed to reduce outlying effects. The fold change concentration of each cytokine and chemokine between the EV-exposed MSCs and the naïve MSCs was evaluated using censored regression. False discovery rates were utilised to adjust for multiple comparisons. Cytokines or chemokines that yielded Luminex assay results that were completely censored for the EV exposed MSCs and/or MSC naïve groups were excluded from the analysis.

Results

NB cells release EVs that stimulate the production of pro-tumorigenic cytokines and chemokines by MSCs by MSCs

We had previously demonstrated that NB cells, which do not produce IL-6, stimulate the production of IL-6 by MSCs in the absence of direct contact with MSCs [26,38]. To determine whether this stimulatory effect was in part mediated by EVs and to explore whether the production of other cytokines and chemokines was stimulated, eqEVs from the serum-free CM of three NB cell lines (SK-N-BE(2), CHLA-255 and NB-19) were collected. These cell lines were initially selected because they differ by the presence of amplification (A) of the MYCN oncogene, SK-N-BE(2) and NB-19 cells being MYCN-A and CHLA-255 cells being MYCN-non-amplified (MYCN-NA). The material obtained was added to cultured MSCs and the media (with/without eqEVs) were screened for the presence of 28 cytokines and chemokines by Luminex 200 immunobead assay/flow cytometry and ELISA (SDF-1/CXCL12, VEGF-A and TGFβ). The data (Figure 1 and Supplemental Figures 2 and 3) revealed a more than two-fold increase in the concentration of IL-5, IL-6, IL-8/CXCL8, IL-1-receptor antagonist (IL-1RA), VEGF, interferon (IFN)-α, MIP-1β/CCL4 and MCP-1/CCL2. In the case of IL-6, IL-8/CXCL8, VEGF and MCP-1/CCL2, the concentrations in the presence of eqEVs of all three cell lines were significantly higher (above 16 pg/ml). SDF-1/CXCL12 production was increased by 1.2-fold (CHLA-255 and SK-N-BE[2]) but this increase was not statistically significant. In contrast, anti-tumorigenic immunomodulatory cytokines like IL-2, IL-7, IL-12, IL-17, TNF-α and Interferon γ were either not detected or their production was not statistically significantly increased upon exposure to eqEVs. A comparative analysis of the protein cargo of eqEVs from these NB cell lines performed by mass spectrometry (Figure 2(a)) identified 92 proteins common to all cell lines (Supplemental Table 1), including several NB markers such as tyrosine 3-mono-oxygenase (Ty3H), secretogranin (SCG)-1 and -3 and chromogranin-A (CHGA), constituent proteins of neurosecretory granules present in NB cells (Figure 2(d)) [39]. An enrichment analysis by cellular component (Figure 2(b)) identified in the three cell lines a higher proportion of proteins present in exosomes (68–70%, $p < 0.01$) and in cytoplasm (67–72%, $p < 0.01$). An enrichment analysis by molecular function (Figure 2(c)) revealed a statistically significant enrichment in extracellular matrix proteins, DNA-binding
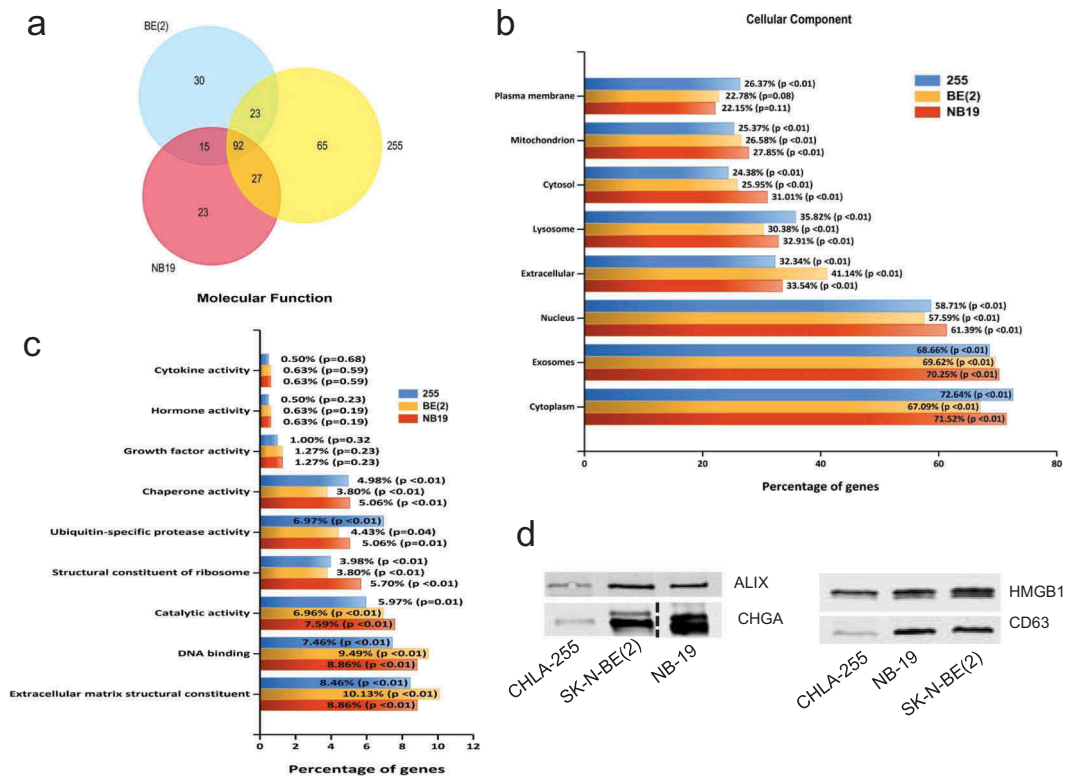
Figure 2. Proteomics analysis of three NB-derived eqEV preparations. eqEV preparations from three human NB cell lines, SK-N-BE[2] (BE[2]), CHLA-255 (255) and NB19 were examined by SDS-PAGE and LC-MS/MS as described in Methods. Data were analysed using the FunRich analysis tool [37]. (a) Venn diagram of all proteins identified in each cell line. (b) Enrichment analysis data according to cellular component. (c) Enrichment analysis data according to molecular function. (d) Western blot analysis of eqEVs for the expression of CD63, HMGB1, ALIX and CHGA.

proteins, catabolic enzymes, ribosome constituents, ubiquitin and chaperon proteins but importantly an absence of enrichment in soluble growth factors, cytokines and hormonal proteins with the exception of high motility group box 1 (HMGB1), a master cytokine regulator [40] whose presence was verified by western blot analysis (Figure 2(d)).

Purification of exosomes from the CM of NB cells

Because EV preparations using ExoQuick-TC have been reported to contain non-EV proteins and do not separate exosomes from other EVs [41], we used three established methods of exosome purification, DUC, ODGC and SEC in parallel [31,32,41] to isolate exosomes from serum-free CM of cultured NB cells (Figure 3). By DUC, we separated precipitates obtained at 2000*g*, 10,000*g* and 100,000*g* and examined them by western blot for the presence of tetraspanins (CD63 and CD81) and ALIX and syntenin [32,33]. This analysis revealed the presence of ALIX and syntenin solely in duc100kEVs pellet, whereas CD63 and CD81 in addition to being present in duc100kEVs were also present in duc2kEVs (apoptotic bodies) and duc10kEVs (MVs) pellets (Figure 3(a)). Using ODGC (Figure 3(b)) we

identified by NTA two peaks rich in particles, one at the top of the gradient (peak 1) and one in fraction 4 (peak 2, density of 1.05 g/ml). This second peak, designated odgcEVs, contained syntenin and ALIX in the absence of calnexin, an endoplasmic reticulum marker and GM130, a mitochondrial marker. The first particle-containing peak contained CHGA. This peak was loaded on a SEC column which separated EVs from CHGA that eluted with the soluble proteins (Supplemental Figure 4(a,b)). This thus demonstrated that CHGA was not associated with EVs but present in a soluble form in the CM of NB cells. This absence of association between CHGA and EVs was confirmed by DUC, which revealed an absence of CHGA not only in duc100kEVs (Supplemental Figure 4) but also in the duc2kEVs and duc10kEVs pellets (Supplemental Figure 4(d)). Using SEC (Figure 3(c)), we isolated syntenin and ALIX containing exosomes in fractions 3 and 4 (secEVs in peak 1) whereas soluble proteins including CHGA eluted in fractions 6–10 (peak 2). The absence of contaminating soluble high molecular weight proteins and protein aggregates in peak 1 was verified by silver staining, confirming that SEC separated EVs from soluble proteins. In contrast to CHGA, Gal-3BP, another soluble protein secreted by NB cells [42], was found to be associated with
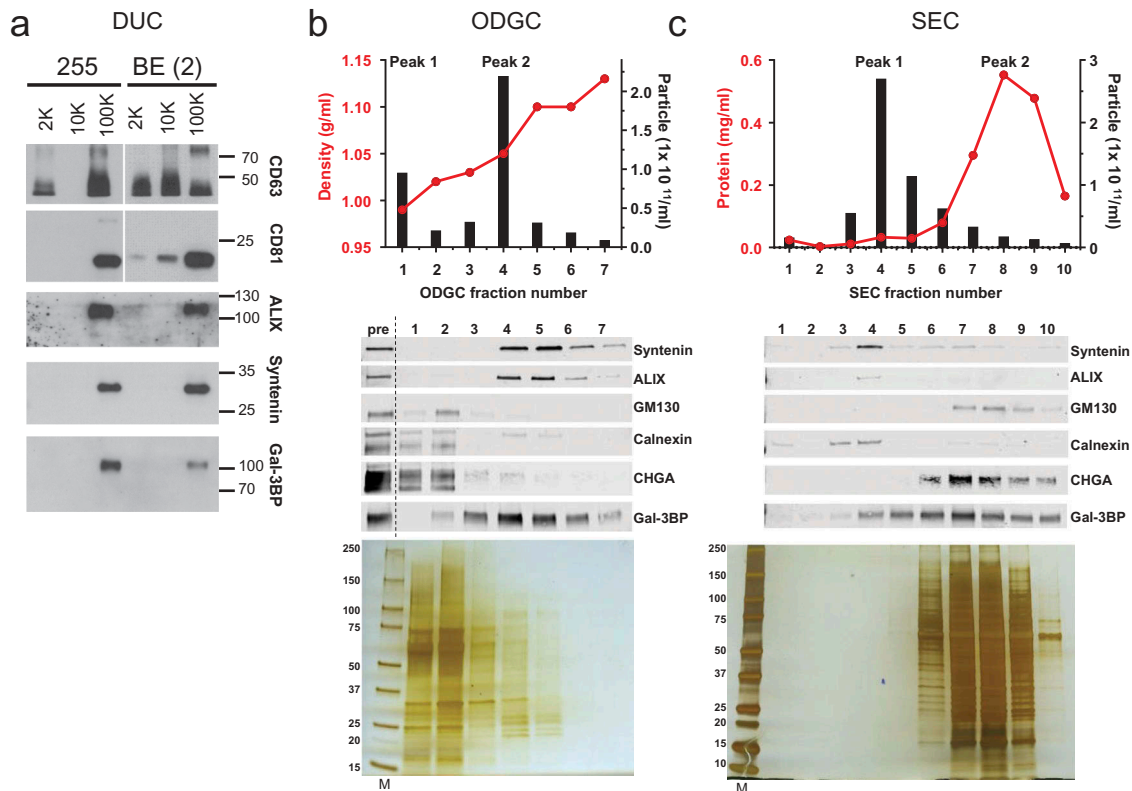
Figure 3. Isolation of NB exosomes by DUC, ODGC and SEC. EVs were collected from the serum-free culture medium of NB cells as indicated in Methods and examined by western blot for the presence of exosomal and non exosomal proteins. (a) Western blot analysis for indicated proteins of duc2kEVs, duc10kEVs and duc100kEVs (1 µg/lane) obtained by DUC of the CM of CHLA-255 (255) and SK-N-BE[2] (BE[2]). (b) Upper: Density and particle number in each fraction obtained by ODGC from the CM of SK-N-BE[2] (BE[2]) cells. Middle: Western Blot analysis of pre (prefractionation) and each fraction analysed by SDS-PAGE (25 µg/lane and 3 µg/lane, respectively). Lower: silver stain of each fraction analysed by SDS-PAGE (10 µl/lane). M, marker. Similar data were obtained with CHLA-255 cells. (c) Upper: Protein concentration and particle number of each fraction obtained by SEC from the CM of SK-N-BE[2] cells. Similar data were obtained with seven other NB cell lines (Figure 7). Middle and Lower: Western blot analysis and silver stain of each fraction analysed by SDS-PAGE (3 µg/lane and 10 µl/lane, respectively). The data are representative of at least three independent experiments showing similar results. Molecular weight standards are indicated (in kDa) on the side of the gels.

duc100kEVs, odgcEVs and secEVs in addition to being present in a soluble form. The presence of exosomes in these preparations was further verified by NTA and TEM. NTA revealed the presence of particles with a mode distribution ranging from 64 to 75 nm (Figure 4(a)) in all three preparations and TEM analysis demonstrated the presence of EVs with a diameter <100 nm (Figure 4(b)), and a morphology consistent with exosomes. Whereas isolation by DUC had a higher yield than ODGC, SEC had a higher yield than the two other methods in the case of CHLA-255 cells (Figure 4(c)).

NB-derived exosomes are captured by MSCs

We then used duc100kEVs labelled with PKH67 and further purified by ODGC to examine EV uptake by MSCs in culture. By fluorescence microscopy, we observed the presence of green fluorescent particles on MSCs after 24 h of incubation (Figure 5(a)). We further demonstrated the uptake of these particles by MSCs by showing the presence of green fluorescent signals inside the cytoplasm of MSCs by confocal microscopy (Figure 5(b,c)). In contrast, liposomes similarly stained were not taken up by MSCs (Figure 5(b)).

NB-derived exosomes stimulate the production of cytokines and chemokines by MSCs

We next tested preparations of duc100kEVs, odgcEVs and secEVs for their ability to stimulate the production of cytokines and chemokines in MSCs. The presence of exosomes in these preparations was verified by western blot analysis for the presence of syntenin and ALIX as well as Gal-3BP and the absence of GM-130 (Figure 6 (a)). These EVs were added to cultured MSCs (2.5–10 µg/3 × 10^4 cells equivalent to 25–100 µg/ml) and the
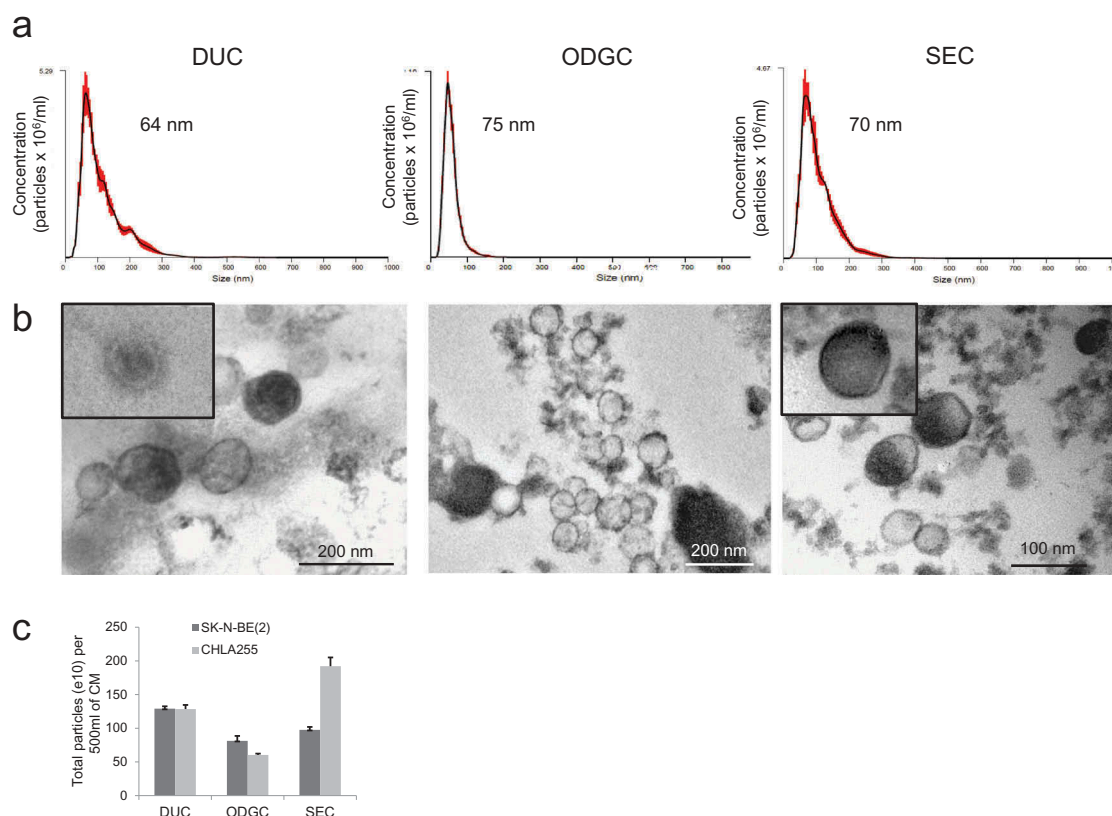
Figure 4. Analysis of NB-derived exosomes by NTA and TEM. (a) Representative concentration vs. size plot by NTA on NB-derived duc100kEVs, odgcEVs and secEVs. The number represents the mode size. (b) Representative TEM pictures of same preparations as in (a) (CHLA-255 for duc100kEVs and secEVs, SK-N-BE[2] for odgcEVs). (c) The amount of EVs obtained from 500 ml of CM from indicated cell lines by the three purification methods was estimated by NTA. The data represents the mean (±SD) particle number from three determinations on a single sample.

culture supernatant was analysed after 24 h for the presence of IL-6, IL-8/CXCL8, MCP-1/CCL2 and VEGF by ELISA. These analyses revealed a dose-dependent increase in the production of cytokines and chemokines by MSCs treated with EVs, with the highest activity seen with secEVs and a higher activity observed with EVs derived from MYCN-A SK-N-BE(2) cells (Figure 6(b)). To determine the relative proportion of IL-6 stimulatory activity associated with EVs and the one associated with soluble proteins, we analysed the supernatant after each DUC step for IL-6 stimulatory activity in the presence of MSCs. This analysis indicated that 69% of the total IL-6 stimulatory activity documented in the 10K supernatant was still present in the 100K supernatant, indicating the presence of activity in soluble proteins. However the activity present in the duc100KEVs only represented 0.95% of the total activity and 0.5% after the duc100KEVs were resuspended and recentrifuged at 100,000g a second time (Supplemental Figure 5(a)), suggesting a loss of activity during the EVs isolation. We then did a comparative analysis between the three purification

methods which indicated that the IL-6 stimulatory activity associated with EVs represented from 0.06 to 3% of the total activity present in the 10,000g supernatant with the highest percentage in secEVs (Supplemental Figure 5(b)). Thus, the data indicate that EV-free medium contains a large proportion of the IL-6 stimulatory activity released by NB cells, and exosomes a relatively small proportion of this activity although some of this activity may be lost during purification. We also tested for IL-6 and IL-8/CXCL8 stimulatory activity, secEVs from an additional six NB cell lines (all derived from patients with metastatic disease) that differ in MYCN-status, disease status (initial vs. progressive), origin (primary tumour vs. metastatic BM) and drug resistance (Figure 7(a,b) and Supplemental Table 2). The data revealed no significant difference between the amount of IL-6 or IL-8/CXCL8 produced by MSCs and the characteristics of the cell lines from which the EVs were derived. We also found that secEVs from MSCs or skin fibroblasts stimulated IL-6 and IL-8/CXCL8 production by MSCs (Supplemental Figure 6), suggesting the presence of
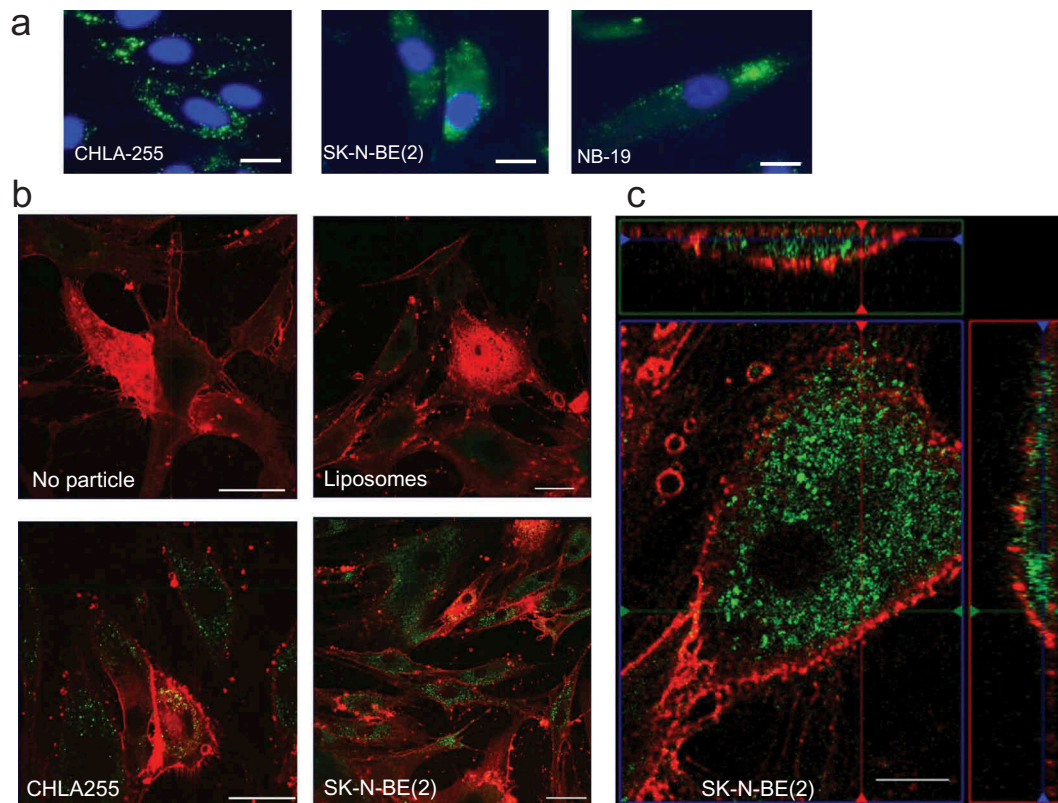
Figure 5. Uptake of NB-derived exosomes by MSCs. (a) Fluorescence microscopy of MSCs (3×10^4/well) after 24 h of incubation in the presence of PKH67-labelled exosomes from three NB cell lines prepared as indicated in Methods. Bar = 20 μm. (b) Confocal microscopy images of MSCs incubated for 24 h in the presence of liposomes, CHLA-255 exosomes or SK-N-BE[2] exosomes labelled with PKH67. MSCs were stained with the red fluorescent membrane dye FM™4-64FX as described in Methods. (c) Same as (b) with green and red boxes representing z sections. Bar = 50 μm in (a) and (b), and 10 μm in (c). The data are representative of three independent experiments showing similar results.

autocrine and paracrine mechanisms where MSCs could also be sensitive to their own exosomes and exosomes produced by non-malignant cells.

The production of IL-6 and IL-8/CXCL8 by NB-derived exosomes is ERK-dependent

To explore the mechanism by which exosomes induce the production of IL-6 and IL-8/CXCL8 by MSCs, we examined in MSCs exposed to SK-N-BE(2) NB-derived secEVs the activation of downstream signalling pathways, including STAT3, NFκB, ERK1/2 and AKT known to be activated by exosomes [43–46]. This experiment (Figure 8(a)) revealed an absence of activation of STAT3 and NFκB but activation of ERK1/2 and AKT within 15 min after exposure to secEVs. We then asked whether activation of these signalling pathways was necessary for the stimulation of IL-6 and IL-8/CXCL8 expression in MSCs by conducting similar experiments in the presence of MK2206 (AKT inhibitor) and trametinib (MEK/ERK inhibitor) (Figure 8 (b)). The data demonstrated that inhibition of ERK1/2 by

trametinib but not AKT by MK2206 prevented the stimulation of IL-6 and IL-8/CXCL8 production in MSCs exposed to SK-N-BE(2) secEVs (Figure 8(c)) and the stimulation of IL-6 by SK-N-SH secEVs (Supplemental Figure 7). Inhibition of ERK1/2 activation by trametinib however did not prevent EV uptake by MSCs, as shown by others [46] (Figure 9).The data thus indicate that the stimulation of IL-6 and IL-8/CXCL8 by exosomes is initiated early upon contact with MSCs, and does not require exosome uptake and release of their content inside MSCs.

Altogether, the data demonstrate that exosomes produced by NB cells contribute with other soluble factors to the polarisation of MSCs towards a pro-tumorigenic function by stimulating in these cells the production of cytokines and chemokines that are favourable to the tumour cells.

Discussion

Our data provide a novel insight into the communication between NB cells and MSCs in the TME,
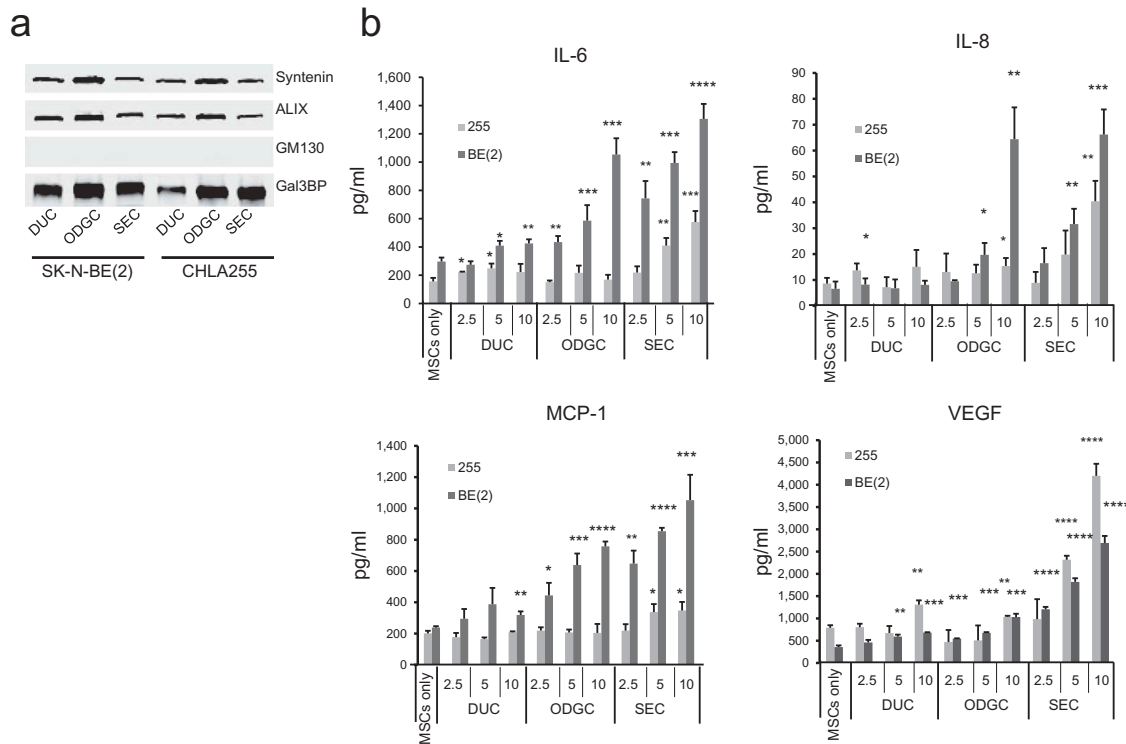
Figure 6. NB-derived exosomes stimulate the production of cytokines and chemokines by MSCs. (a) Western blot (4 µg/lane) analysis of the three preparations used in (b). (b) MSCs (3 × 10⁴/well in 100 µl of serum-free culture medium) were exposed for 24 h to indicated amount of NB-derived duc100kEVs, odgcEVs and secEVs as shown in Figures 3 and 4. The culture medium was then analysed for the presence of IL-6, IL-8/CXCL8, MCP-1/CCL2, and VEGF by ELISA. The data represent the mean (±SD) values in pg/ml of triplicate samples from one experiment and are representative of two independent experiments showing similar results. The *p*-values are between untreated (MSCs only) and exosome-treated MSCs. ****p < 0.0001, ***p < 0.001, **p < 0.01 and *p < 0.05.
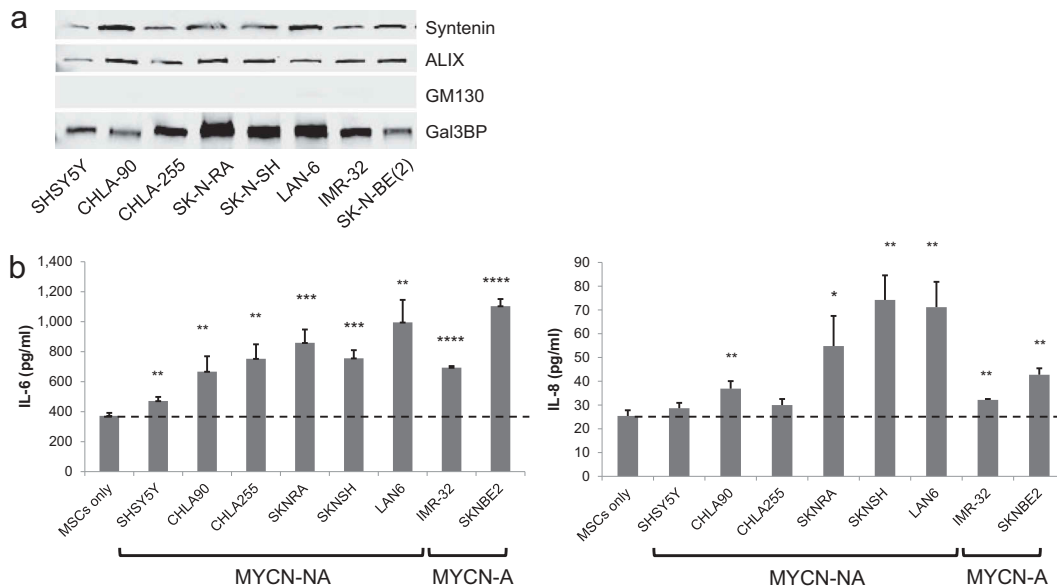

Figure 7. Stimulation of IL-6 and IL-8/CXCL8 in MSCs by exosomes from eight NB-cell lines. (a) Western blot analysis of secEVs (2.5 µg/lane) from indicated cell lines. (b) secEVs were added to cultured MSCs (5.0 µg/3 × 10⁴ cells) and the medium was analysed after 24 h for IL-6 and IL-8/CXCL8 concentrations by ELISA. The data represent the mean (±SD) concentrations from triplicate samples in a single experiment. MYCN status is indicated at the bottom (NA = non-amplified; A = amplified) and the characteristics of the cell lines are shown in Supplemental Table 2. The *p*-values are between untreated (MSCs only) and exosome-treated MSCs. ****p < 0.0001, ***p < 0.001, **p < 0.01 and *p < 0.05.
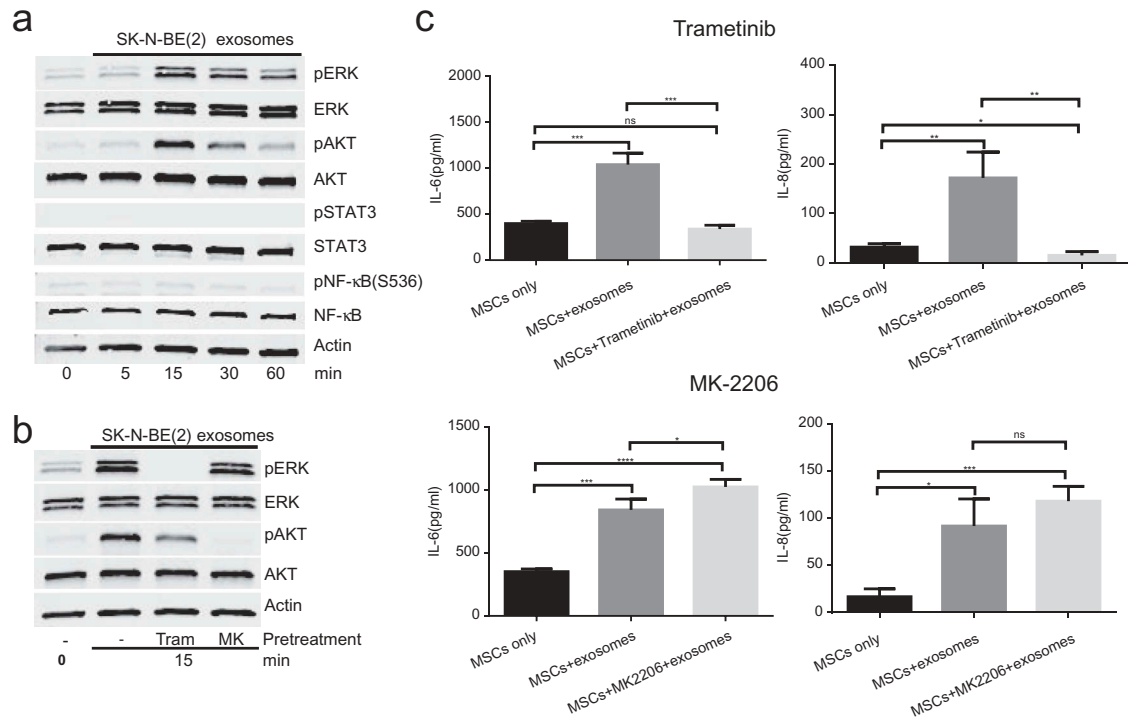
Figure 8. Stimulation of IL-6 and IL-8/CXCL8 production by NB-derived exosomes is ERK-dependent. (a) MSCs were exposed to SK-N-BE[2]-derived secEVs (50 μg/ml) obtained by SEC and cell lysates collected at indicated times were examined by western blot (15 μg/lane) for the presence of STAT3, ERK1/2, AKT, NFκB (p65) and their phosphorylated forms. Actin was used as a loading control. (b) MSCs were pre-treated for 2 h with MK-2206 (MK, 1 μM) or trametinib (Tram, 1 μM) prior to being treated with SK-N-BE[2]-derived secEVs as in (a). Cell lysates were obtained after 15 min and examined by western blot (15 μg/lane) for the expression of AKT and ERK1/2 and their phosphorylated forms. Actin was used as a loading control. (c) MSCs were pre-treated with trametinib or MK-2206 as in (b) before being exposed to SK-N-BE[2]-derived secEVs as in (a) and (b), and the concentration of IL-6 and IL-8/CXCL8 in the culture medium was determined after 24 h by ELISA. The data represent the mean (±SD) concentration of triplicate samples and are representative of two independent experiments showing similar results. ****$p < 0.0001$, ***$p < 0.001$, **$p < 0.01$, *$p < 0.1$. ns: non-significant.
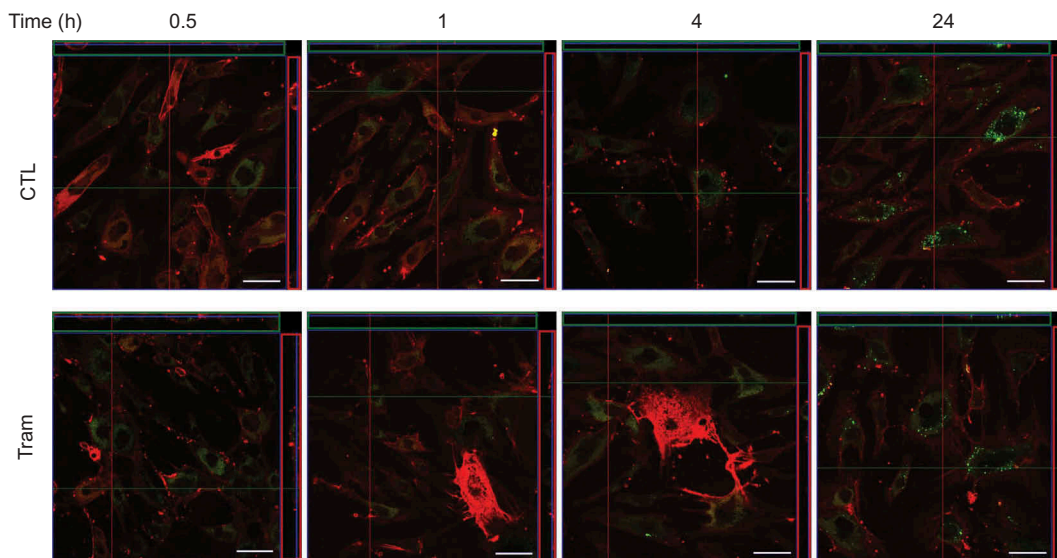

Figure 9. Inhibition of ERK1/2 does not prevent exosome uptake by MSCs. MSCs were incubated in the absence or presence of trametinib (1 μM) 2 h before the addition of PKH-67-labelled SK-N-BE[2]-derived exosomes (5×10^9 particles/ml) and examined at indicated times for exosome uptake by confocal microscopy as shown in Figure 5. Scale bar = 50 μm.

pointing to a mechanism by which tumour cells activate MSCs to release pro-tumorigenic factors. Our analysis of chemokine and cytokine expression by MSCs exposed to NB-derived exosomes revealed an increased production of factors seen in chronic inflammation and having a direct effect on tumour cell proliferation and survival, on angiogenesis and on the recruitment of other inflammatory cells that favour tumour cells and their progression [47]. The pro-tumorigenic effect of IL-6 has been well demonstrated by many laboratories, including ours, as IL-6 stimulates tumour cell proliferation [38,48], increases bone metastasis [26], protects tumour cells from apoptosis and promotes drug resistance [49]. IL-8/CXCL8 and VEGF have a known stimulatory effect on tumour vascularisation and angiogenesis [50] and intracellular VEGF in MSCs stimulate their maturation into osteoblasts [51]. MCP-1/CCL2 promotes the recruitment of macrophages into tumours and their polarisation into Th2-driven tumour-associated macrophages by GM-CSF [52]. SDF-1/CXCL12 is a chemoattractant for metastatic tumour cells [53]. In contrast, there was an absence of effect on the production of immunostimulatory or anti-tumorigenic cytokines such as IFNγ, GM-CSF, IL-2, IL-7, IL-12 or IL-17 [54]. Similar effects of exosomes on the production of chemokines and cytokines by stromal cells in the TME have been reported in other types of cancer. Exosomes derived from chronic lymphocytic leukaemia cells induce the transition of MSCs into tumour-associated fibroblasts and the production of multiple pro-tumorigenic chemokines including IL-6 and IL-8/CXCL8, anti-apoptotic factors and migration/invasion-related factors [55]. Lung cancer-derived exosomes induce the production of IL-6, IL-8/CXCL8 and MCP-1/CCL2 in MSCs in an NFκB and Toll-like receptor 2-dependent mechanism [56]. Glioblastoma and other tumour-derived exosomes induce the production of IL-6 and VEGF by monocytes/macrophages and endothelial cells [57,58].

Our comparative analysis of eight NB cell lines did not provide evidence for a relation between the stimulatory activity of NB exosomes on IL-6 and IL-8/CXCL8 production by MSCs and some of the characteristics of the NB cell lines such as amplification of the MYCN oncogene, drug resistance, origin of the cell line or disease progression. This is not entirely unexpected as all cell lines were derived from patients with stage 4 (metastatic) disease. The data also need to be cautiously interpreted because of the limited number of cell lines examined and the sole focus on IL-6 and IL-8/CXCL8 stimulation. It is also interesting to note that non-malignant cells like fibroblasts and MSCs produce exosomes

that stimulate the production of IL-6 and IL-8/CXCL8 in MSCs, indicating the presence of paracrine and autocrine mechanisms of stimulation also in normal cells.

Our data demonstrate that although exosomes are active in stimulating the production of cytokines and chemokines by MSCs, they require concentrations in the 25–100 μg/ml range to be active and their activity represents a small fraction of the total stimulatory activity present in the CM of NB cells. The fact that NB exosomes are active at concentrations in the μg/ml range in contrast to soluble growth factors and chemokines that are typically active at concentrations in the pg/ml range is anticipated, considering that the cargo of exosomes contains a large amount of proteins. Similar concentrations of exosomes from chronic lymphocytic leukaemia cells were reported to be needed to activate kinases in MSCs and endothelial cells [55] or for exosomes from A549 lung carcinoma cells to stimulate the production of inflammatory cytokines by MSCs [56]. Tumour-derived exosome concentrations of 100 μg/ml were needed to stimulate hypoxia-mediated activation of endothelial cells [59]. In contrast to soluble cytokines and chemokines, exosomes have a broader spectrum of activity because of the diversity of regulatory molecules present in their cargo, including micro RNA [60–62]. Another important aspect is the potentially important difference in *in vivo* activity. In contrast to soluble cytokines, whose activity is typically cell-specific, exosomes have a specific organotropism as recently suggested [63] and thus have the potential to target several cell types in a specific organ, orchestrating multiple biological changes. The fact that exosomes represent only a small proportion of the total activity detected in the CM of NB cells (Supplemental Table 2) is another important observation. This analysis confirmed that soluble proteins present in the CM of NB cells contribute to the stimulation of IL-6 in MSCs. We had for example previously reported that Gal-3BP present in the CM of NB cells stimulates IL-6 expressions in MSCs [42,64]. The exact contribution of exosomes to this activity is however difficult to precisely determine as activity is further lost during the purification and isolation of exosomes. This may in part be due to the method of purification. Purification methods that include ultracentrifugation like DUC and ODGC have been reported to cause damage to the exosome membrane, and this is consistent with the fact that exosomes prepared by SEC, a method that did not include centrifugation at high speed, had the highest activity [65].

Our data also provide insight into the importance of the method used to isolate EVs, and in particular the use of commercially available precipitation methods such as

ExoQuick-TC [41]. This is illustrated by our observation that CHGA, identified by proteomics analysis on eqEVs was found not to be associated with exosomes but present in a soluble form as shown in preparations of EVs obtained by DUC, ODGC or SEC. Thus in NB, CHGA is secreted from secretory granules present in NB cells [39] and is not associated in EVs as is seen in prostasome released by prostate and prostate cancer cells [66].

In contrast to CHGA, Gal-3BP, another protein secreted by NB cells, was associated with all three exosome-rich preparations (duc100kEVs, odgcEVs and secEVs) in addition to being present in a soluble form. Gal-3BP is a sialoglycoprotein often present in exosomes from normal and cancer cells [67,68] and is among the 100 most common proteins reported in the ExoCarta database (http://www.exocarta.org). It is also among the 25 common cancer proteins associated with EVs secretion and identified in all NCI-60 cancer cell lines [69]. Its role in exosome biology and activity is presently unknown. Gal-3BP interacts with Gal-3 present at the cell surface of MSCs and transcriptionally upregulates the production of IL-6 in a RAS/MEK/ERK-dependent manner [41]. It is thus conceivable that its presence at the surface of exosomes plays a similar role.

Finally, we demonstrate that ERK1/2 inhibition prevents the stimulation of IL-6 and IL-8/CXCL8 by exosomes, without affecting exosome uptake. It thus suggests that release of IL-6 and IL-8/CXCL8 by MSCs is the result of an early signalling event upon contact between a protein present at the surface of exosomes acting as a ligand and a protein present in MSCs acting as a receptor. Gal-3BP, which we show to be associated with NB-derived exosomes, could be such a ligand and this possibility is currently examined in our laboratory.

Author's contributions

RN performed most of the experiments described; HS performed the EM analysis (Figure 4(b)); GEF contributed to the data shown in Figures 5 and 9; RF generated the data shown in Figure 2; MF provided input on the methods and critically reviewed the manuscript; JM assisted with the statistical analysis of the data; PZ provided reagents, assistance in the methodologies and critically reviewed the manuscript; YAD conceived and coordinated the study, reviewed the data and the design of the experiments, and wrote the paper. All authors approved the final submission of the manuscript.

ORCID

Rob Fanter 🔵 http://orcid.org/0000-0003-2981-4182
Jemily Malvar 🔵 http://orcid.org/0000-0002-5481-6780
Pascale Zimmermann 🔵 http://orcid.org/0000-0001-8768-1790
Yves A. DeClerck 🔵 http://orcid.org/0000-0002-3688-0113

References

[1] Boulais PE, Frenette PS. Making sense of hematopoietic stem cell niches. Blood. 2015;125(17):2621–2629.

[2] Psaila B, Lyden D. The metastatic niche: adapting the foreign soil. NatRevCancer. 2009;9(4):285–293.

[3] Meads MB, Hazlehurst LA, Dalton WS. The bone marrow microenvironment as a tumor sanctuary and contributor to drug resistance. Clin Cancer Res. 2008;14(9):2519–2526.

[4] Lam HM, Vessella RL, Morrissey C. The role of the microenvironment-dormant prostate disseminated tumor cells in the bone marrow. Drug Discov Today Technol. 2014;11:41–47.

[5] Sosa MS, Bragado P, Aguirre-Ghiso JA. Mechanisms of disseminated cancer cell dormancy: an awakening field. Nat Rev Cancer. 2014;14(9):611–622.

[6] Phinney DG, Prockop DJ. Concise review: mesenchymal stem/multipotent stromal cells: the state of transdifferentiation and modes of tissue repair–current views. Stem Cells. 2007;25(11):2896–2902.

[7] Bergfeld SA, DeClerck YA. Bone marrow-derived mesenchymal stem cells and the tumor microenvironment. Cancer Metastasis Rev. 2010;29(2):249–261.

[8] Barcellos-de-Souza P, Gori V, Bambi F, et al. Tumor microenvironment: bone marrow-mesenchymal stem cells as key players. Biochim Biophys Acta. 2013;1836(2):321–335.

[9] Karnoub AE, Dash AB, Vo AP, et al. Mesenchymal stem cells within tumour stroma promote breast cancer metastasis. Nature. 2007;449(7162):557–563.

[10] Bergfeld SA, Blavier L, DeClerck YA. Bone marrow-derived mesenchymal stromal cells promote survival and drug resistance in tumor cells. Mol Cancer Ther. 2014;13(4):962–975.

[11] Bernardo ME, Fibbe WE. Mesenchymal stromal cells: sensors and switchers of inflammation. Cell Stem Cell. 2013;13(4):392–402.

[12] Krampera M. Mesenchymal stromal cell 'licensing': A multistep process. Leukemia. 2011;25(9):1408–1414.

[13] van der Pol E, Boing AN, Harrison P, et al. Classification, functions, and clinical relevance of extracellular vesicles. Pharmacol Rev. 2012;64(3):676–705.

[14] Yanez-Mo M, Siljander PR, Andreu Z, et al. Biological properties of extracellular vesicles and their physiological functions. J Extracell Vesicles. 2015;4:27066.

[15] Harding CV, Heuser JE, Stahl PD. Exosomes: looking back three decades and into the future. J Cell Biol. 2013;200(4):367–371.

[16] Colombo M, Raposo G, Thery C. Biogenesis, secretion, and intercellular interactions of exosomes and other extracellular vesicles. Annu Rev Cell Dev Biol. 2014;30:255–289.

[17] Vader P, Breakefield XO, Wood MJ. Extracellular vesicles: emerging targets for cancer therapy. Trends Mol Med. 2014;20(7):385–393.

[18] Tkach M, Thery C. Communication by extracellular vesicles: where we are and where we need to go. Cell. 2016;164(6):1226–1232.

[19] Whiteside TL. Immune modulation of t-cell and nk (natural killer) cell activities by texs (tumour-derived exosomes). Biochem Soc Trans. 2013;41(1):245–251.

[20] Bobrie A, Thery C. Exosomes and communication between tumours and the immune system: are all exosomes equal? Biochem Soc Trans. 2013;41(1):263–267.

[21] Grange C, Tapparo M, Collino F, et al. Microvesicles released from human renal cancer stem cells stimulate angiogenesis and formation of lung premetastatic niche. Cancer Res. 2011;71(15):5346–5356.

[22] Hood JL, San RS, Wickline SA. Exosomes released by melanoma cells prepare sentinel lymph nodes for tumor metastasis. Cancer Res. 2011;71(11):3792–3801.

[23] Peinado H, Aleckovic M, Lavotshkin S, et al. Melanoma exosomes educate bone marrow progenitor cells toward a pro-metastatic phenotype through met. Nat Med. 2012;18(6):883–891.

[24] Dubois SG, Kalika Y, Lukens JN, et al. Metastatic sites in stage iv and ivs neuroblastoma correlate with age, tumor biology, and survival. J Pediatr Hematol Oncol. 1999;21(3):181–189.

[25] Maris JM. Recent advances in neuroblastoma. N Engl J Med. 2010;362(23):2202–2211.

[26] Sohara Y, Shimada H, Minkin C, et al. Bone marrow mesenchymal stem cells provide an alternate pathway of osteoclast activation and bone destruction by cancer cells. Cancer Res. 2005;65(4):1129–1135.

[27] Horwitz EM, Le Blanc K, Dominici M, et al. Clarification of the nomenclature for msc: the international society for cellular therapy position statement. Cytotherapy. 2005;7(5):393–395.

[28] Krampera M, Galipeau J, Shi Y, et al. Immunological characterization of multipotent mesenchymal stromal cells–the international society for cellular therapy (isct) working proposal. Cytotherapy. 2013;15(9):1054–1061.

[29] Kashyap R, Roucourt B, Lembo F, et al. Syntenin controls migration, growth, proliferation, and cell cycle progression in cancer cells. Front Pharmacol. 2015;6:241.

[30] Li J, Lee Y, Johansson HJ, et al. Serum-free culture alters the quantity and protein composition of neuroblastoma-derived extracellular vesicles. J Extracell Vesicles. 2015;4:26883.

[31] Boing AN, Van Der Pol E, Grootemaat AE, et al. Single-step isolation of extracellular vesicles by size-exclusion chromatography. J Extracell Vesicles. 2014;3:23430.

[32] Kowal J, Arras G, Colombo M, et al. Proteomic comparison defines novel markers to characterize heterogeneous populations of extracellular vesicle subtypes. Proc Natl Acad Sci U S A. 2016;113(8):E968–77.

[33] Ghossoub R, Lembo F, Rubio A, et al. Syntenin-alix exosome biogenesis and budding into multivesicular bodies are controlled by arf6 and pld2. Nat Commun. 2014;5:3477.

[34] Lotvall J, Hill AF, Hochberg F, et al. Minimal experimental requirements for definition of extracellular vesicles and their functions: A position statement from the international society for extracellular vesicles. J Extracell Vesicles. 2014;3:26913.

[35] Mathivanan S, Simpson RJ. Exocarta: A compendium of exosomal proteins and rna. Proteomics. 2009;9 (21):4997–5000.

[36] Kim DK, Kang B, Kim OY, et al. Evpedia: an integrated database of high-throughput data for systemic analyses of extracellular vesicles. J Extracell Vesicles. 2013;2:20384.

[37] Pathan M, Keerthikumar S, Ang CS, et al. Funrich: an open access standalone functional enrichment and interaction network analysis tool. Proteomics. 2015;15 (15):2597–2601.

[38] Ara T, Song L, Shimada H, et al. Interleukin-6 in the bone marrow microenvironment promotes the growth and survival of neuroblastoma cells. Cancer Res. 2009;69 (1):329–337.

[39] Weiler R, Meyerson G, Fischer-Colbrie R, et al. Divergent changes of chromogranin a/secretogranin ii levels in differentiating human neuroblastoma cells. FEBS Lett. 1990;265(1–2):27–29.

[40] Harris HE, Andersson U, Pisetsky DS. Hmgb1: A multifunctional alarmin driving autoimmune and inflammatory disease. Nat Rev Rheumatol. 2012;8(4):195–202.

[41] Van Deun J, Mestdagh P, Sormunen R, et al. The impact of disparate isolation methods for extracellular vesicles on downstream rna profiling. J Extracell Vesicles. 2014;3:34858.

[42] Silverman AM, Nakata R, Shimada H, et al. A galectin-3-dependent pathway upregulates interleukin-6 in the microenvironment of human neuroblastoma. Cancer Res. 2012;72(9):2228–2238.

[43] Chalmin F, Ladoire S, Mignot G, et al. Membrane-associated hsp72 from tumor-derived exosomes mediates stat3-dependent immunosuppressive function of mouse and human myeloid-derived suppressor cells. J Clin Invest. 2010;120(2):457–471.

[44] Fabbri M, Paone A, Calore F, et al. Micrornas bind to toll-like receptors to induce prometastatic inflammatory response. Proc Natl Acad Sci USA. 2012;109(31): E2110–E6.

[45] Liu S, Sun J, Lan Q. Glioblastoma microvesicles promote endothelial cell proliferation through akt/beta-catenin pathway. Int J Clin Exp Pathol. 2014;7(8):4857–4866.

[46] Svensson KJ, Christianson HC, Wittrup A, et al. Exosome uptake depends on erk1/2-heat shock protein 27 signaling and lipid raft-mediated endocytosis negatively regulated by caveolin-1. J Biol Chem. 2013;288 (24):17713–17724.

[47] Munn LL. Cancer and inflammation. Wiley Interdiscip Rev Syst Biol Med. 2016;9(8):DOI: 10.1002/wsbm.1370.

[48] Rossi JF, Lu ZY, Jourdan M, et al. Interleukin-6 as a therapeutic target. Clin Cancer Res. 2015;21(6):1248–1257.

[49] Ara T, Nakata R, Sheard MA, et al. Critical role of stat3 in il-6-mediated drug resistance in human neuroblastoma. Cancer Res. 2013;73(13):3852–3864.

[50] Ferrara N. Role of vascular endothelial growth factor in physiologic and pathologic angiogenesis: therapeutic implications. SeminOncol. 2002;29(6 Suppl 16):10–14.

[51] HaDuong JH, Blavier L, Baniwal SK, et al. Interaction between bone marrow stromal cells and neuroblastoma cells leads to a vegfa-mediated osteoblastogenesis. Int J Cancer. 2015;137(4):797–809.

[52] Sierra-Filardi E, Nieto C, Dominguez-Soto A, et al. Ccl2 shapes macrophage polarization by gm-csf and m-csf: identification of ccl2/ccr2-dependent gene expression profile. J Immunol. 2014;192(8):3858–3867.

[53] Wang J, Loberg R, Taichman RS. The pivotal role of cxcl12 (sdf-1)/cxcr4 axis in bone metastasis. Cancer Metastasis Rev. 2006;25(4):573–587.

[54] Vacchelli E, Eggermont A, Fridman WH, et al. Trial watch: immunostimulatory cytokines. Oncoimmunology. 2013;2 (7):e24850.

[55] Paggetti J, Haderk F, Seiffert M, et al. Exosomes released by chronic lymphocytic leukemia cells induce the transition of stromal cells into cancer-associated fibroblasts. Blood. 2015;126(9):1106–1117.

[56] Li X, Wang S, Zhu R, et al. Lung tumor exosomes induce a pro-inflammatory phenotype in mesenchymal stem cells via nfkappab-tlr signaling pathway. J Hematol Oncol. 2016;9:42.

[57] De Vrij J, Maas SL, Kwappenberg KM, et al. Glioblastoma-derived extracellular vesicles modify the phenotype of monocytic cells. Int J Cancer. 2015;137 (7):1630–1642.

[58] Al-Nedawi K, Meehan B, Kerbel RS, et al. Endothelial expression of autocrine vegf upon the uptake of tumor-derived microvesicles containing oncogenic egfr. Proc Natl Acad Sci U S A. 2009;106(10):3794–3799.

[59] Kucharzewska P, Christianson HC, Welch JE, et al. Exosomes reflect the hypoxic status of glioma cells and mediate hypoxia-dependent activation of vascular cells during tumor development. Proc Natl Acad Sci U S A. 2013;110(18):7312–7317.

[60] Melo SA, Sugimoto H, O'Connell JT, et al. Cancer exosomes perform cell-independent microrna biogenesis and promote tumorigenesis. Cancer Cell. 2014;26 (5):707–721.

[61] Challagundla KB, Wise PM, Neviani P, et al. Exosome-mediated transfer of micrornas within the tumor microenvironment and neuroblastoma resistance to chemotherapy. J Natl Cancer Inst. 2015;107:7.

[62] Skog J, Wurdinger T, Van Rijn S, et al. Glioblastoma microvesicles transport rna and proteins that promote tumour growth and provide diagnostic biomarkers. Nat Cell Biol. 2008;10(12):1470–1476.

[63] Hoshino A, Costa-Silva B, Shen TL, et al. Tumour exosome integrins determine organotropic metastasis. Nature. 2015;527(7578):329–335.

[64] Fukaya Y, Shimada H, Wang LC, et al. Identification of gal-3 binding protein as a factor secreted by tumor cells that stimulates interleukin-6 expression in the bone marrow stroma. J Biol Chem. 2008;283(27):18573–18581.

[65] Taylor DD, Shah S. Methods of isolating extracellular vesicles impact down-stream analyses of their cargoes. Methods. 2015;87:3–10.

[66] Carlsson L, Nilsson O, Larsson A, et al. Characteristics of human prostasomes isolated from three different sources. Prostate. 2003;54(4):322–330.

[67] Escrevente C, Grammel N, Kandzia S, et al. Sialoglycoproteins and n-glycans from secreted exosomes of ovarian carcinoma cells. Plos One. 2013;8(10):e78631.

[68] Block AS, Saraswati S, Lichti CF, et al. Co-purification of mac-2 binding protein with galectin-3 and association with prostasomes in human semen. Prostate. 2011;71(7):711–721.

[69] Hurwitz SN, Rider MA, Bundy JL, et al. Proteomic profiling of nci-60 extracellular vesicles uncovers common protein cargo and cancer type-specific biomarkers. Oncotarget. 2016;7(52):86999–87015.